A Single-Station Ionospheric Forecast Model with LSTM Considering Multiple Factors

Ting Xie, Zhiqiang Dai(✉), and Xiangwei Zhu

Sun Yat-Sen University School of Electronics and Communication Engineering, Shenzhen, China
daizhiqiang@mail.sysu.edu.cn

Abstract. The purpose of this study is to verify the rationality and validity of directly adopting segmental modeling prediction of single-station regional scatter data by considering space environment information comprehensively. First, a single-station regional ionospheric model is constructed and predicted by the long short-term memory neural network (LSTM) method based on the single-station global positioning system total electron content (GPS-TEC) data of different regions (low-, mid-, and high latitude regions) and the space environment data. Then, the prediction results are compared and analyzed with the international reference ionosphere 2016 (IRI2016) model, CMONOC Regional Ionosphere Maps (RIM) data, and GPS measurement data. The results show that: i) the LSTM model forecasts are consistent with GPS-TEC observations at high, mid and low latitudes, and the forecast error is less than 3 TECu. The forecast accuracy is much better than that of the IRI2016 model and RIM TEC, and is less susceptible to anomalies. Geographically, the forecast MAE and RMSE of LSTM model decreases with increasing latitude. Among them, the relative accuracy of LSTM forecasts in low and mid latitudes is high, up to 82% or more; ii) the RIM data as a whole are more consistent with the measured data, but the RIM TEC is overestimated during the daytime, a phenomenon related to the discrete anomalies; iii) the IRI2016 model only captures the general trend of TEC. The IRI model forecast values are poor in daytime forecasting, and its overestimation becomes more obvious as the latitude increases, while the forecast performance is better in the evening. This study is a foundation for subsequent regional modeling and forecasting of the ionosphere, and can provide ionospheric constraints to support navigation positioning.

Keywords: LSTM · Single-station VTEC model · RIM · IRI2016 · Accuracy comparison

1 Introduction

The ionosphere is an ionized region in the Earth's upper atmosphere, mainly distributed in the range of about 60–1000 km from the ground. Radio communication systems, satellite navigation and positioning systems, radar detection systems, etc. pass through the ionosphere during signal propagation, which in turn will produce signal delay, signal

C. Yang and J. Xie (Eds.): *China Satellite Navigation Conference (CSNC 2022) Proceedings*, LNEE 910, pp. 230–240, 2022.
https://doi.org/10.1007/978-981-19-2576-4_20

refraction, etc. This ultimately affects satellite-based navigation, positioning, timing and communication services [1–3]. Secondly, abnormal ionospheric changes are closely related to the space environment and the Earth's activities. Monitoring and prediction of TEC is of great practical and academic value since the total ionospheric electric content (TEC) is a quantitative indicator to characterize the ionosphere.

In recent years, scholars have proposed many optimized ionospheric TEC prediction models, which can be divided into two main categories as follows. The first is empirical ionospheric models, such as the Klobuchar model [4, 5], NeQuick model [6, 7], and one of the most widely used models is the IRI model [8, 9]. The other type is the statistical modeling approach for measurement data, which mathematically models TEC time series with high accuracy. Specifically, these include ARMA models [10–12], neural networks [13–17], etc. Given the ability of neural networks to describe complex nonlinear input-output relations, more and more scholars have recently used neural networks for forecasting ionospheric parameters, mainly including radial basis functions (RBF) [13], convolutional NN (CNN) [14], and long short-term memory [15–17] (LSTM).

The process of the above prediction methods is basically: first, a single point time series is obtained by modeling the scattered measurement data in a certain period using polynomial or spherical harmonic models. Then, different mathematical methods are used to make predictions based on this time series, or directly based on the IGS ionospheric grid data. These methods cannot perform simultaneous modeling and forecasting of the single-station ionosphere based on the original measured data, losing some spatial features of the ionosphere and artificially introducing modeling errors. Therefore, in this paper, the segmental modeling method is introduced into the LSTM network, and the ionospheric scatter data over a fixed period of multiple days are directly used to construct the network model. On the other hand, the ionosphere is sensitive to solar activity and changes in near-Earth space, and has complex spatial and temporal distribution characteristics. Its distribution characteristics depend on a variety of factors such as geographical location (polar and auroral zones, high latitudes and equatorial regions), solar activity levels, and geomagnetic activity conditions. It is difficult to describe the high dynamics of the ionosphere by only single-factor modeling. Therefore, this paper constructs a single-station regional model of ionospheric TEC based on TEC data from a single GPS station pierce point and uses an LSTM network suitable for time-series feature learning to forecast ionospheric TEC values for the next 24 h using historical TEC data, solar activity index and geomagnetic activity index as model inputs. And the parameter adaptive method is used to reduce the ionospheric forecast error and improve the generalization ability of the model, to establish an accurate single-station TEC regional model and forecast model.

2 Data Collection and Preprocessing

To better represent the modeling and prediction results of the model, this paper selects the data set during the high solar activity year 2014, i.e., January 1 to January 17 (as shown in Fig. 1).

TEC Dataset: For one of the datasets, the ground-based station actual measurement data from the China Continental Tectonic Environment Monitoring Network

(CMONOC) are used in this paper. Using the GPS dual-frequency data, the carrier phase smoothing pseudorange method was used to solve the single-point VTEC values, and the calculated expressions are shown in Eqs. 1 and 2. The final adopted VTEC data time interval is 30 s, and the thin layer height of ionosphere is 350 km.

$$VTEC = -\frac{\cos z'}{40.28}\frac{f_1^2 f_2^2}{f_1^2 - f_2^2}\left[\tilde{P}_4 - \left(\mathrm{DCB}^S + \mathrm{DCB}^r\right)\right] \tag{1}$$

$$\tilde{P}_4(t) = \overline{P}_4(t) + \Delta L_4(t) = \overline{P}_4(t) + L_4(t) - \overline{L}_4(t) \tag{2}$$

where $P_4 = P_2 - P_1$, $L_4 = L_2 - L_1$, $P_i(t)$ is the carrier phase observation at time t (i takes 1 and 2); L_i is the phase observation corresponding to that epoch; $\overline{L}_i$ is the average value of the carrier phase observation; $\overline{P}_4$ is the average value of the pseudorange observation; DCB^S and DCB^r are the differential code bias of the satellite and receiver, respectively, which can be corrected directly by using the P1-C1 and P1-P2 files of the CODE Center.

The Regional Ionosphere Maps (RIM) data released by CMONOC are directly used in this paper to compare with the LSTM model predictions. The temporal resolution of the RIM data is 2 h. The spatial coverage is from latitude 15.0°N to 55.0°N, longitude 70.0°E to 140.0°E, and the spatial resolution is 1° × 1°. The IRI model [6] is an internationally recognized and recommended standard for the climate specification of ionospheric parameters. To test the ability of the IRI model to predict TEC and verify the forecasting performance of the LSTM model, the latest IRI2016 online version data is used in this paper for a comparative study (https://ccmc.gsfc.nasa.gov/modelweb/models/iri2016_vitmo.php), where the upper height limit is set to 2000 km and the thin layer height is set to 350 km.

Space Environment Dataset: The data were screened for correlation using Pearson correlation coefficient method and Fréchet method [19] before data selection to ensure that the data were weakly correlated with each other. After screening, the datasets characterizing the solar activity: sunspot number SSN, 10.7 cm radio flux F10.7, and the geomagnetic activity level index Ap and magnetic storm ring current index Dst characterizing the Earth's activity were selected.

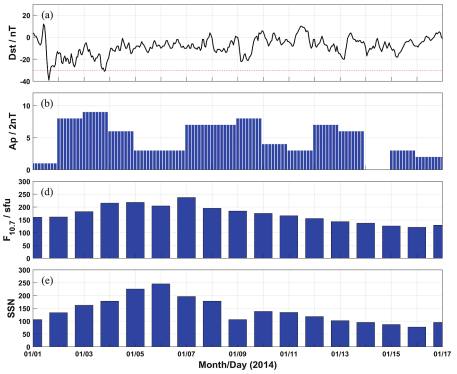

Fig. 1. Space environment data in the selected time period

3 LSTM Neural Network Modeling Method

LSTM is a special type of recursive neural network that captures the most important features from time series data and performs association modeling.

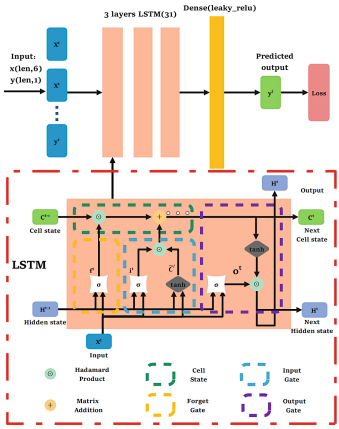

Fig. 2. Structure of LSTM neural network

The structure of the LSTM neural network model is shown in Fig. 2. With a stacked LSTM with three hidden layers, Adam algorithm as the optimizer, and an MSE as the loss function, the input to the model is a continuous 30-min single-station historical observation data. In this paper, three LSTM layers are used, and the number of training times is fixed to 50. The early stop method is used to monitor the validation set loss value (val_loss), where the patience is set to 3. The depth size of each layer is changed for cyclic testing, and the number of hidden layer units that make the training set loss value (loss) and var_loss value optimal is selected. This paper sets the number of hidden layer units to 31, and the Leaky_ReLU activation function is used for the fully connected layer (Dense). This is to avoid the problem of gradient jaggedness in the direction of the gradient by calculating the gradient even if the input of the Leaky_ReLU activation function is less than zero in the back propagation process.

In this paper, single-station GPS data of different latitudes are used for modeling experiments, and the modeling process is shown in Fig. 3. The specific process is as follows: i) the weakly correlated geomagnetic data and solar activity data set are screened using Pearson and Fréchet methods; ii) the single-station GPS data are pre-processed, i.e., the VTEC value, longitude and latitude of the ionospheric pierce point are calculated; iii) the above data are integrated, and the input data sets are: Ap, Dst, F107, SSN, longitude, and latitude. The data sets are divided into 30-min intervals, a total of 48 data sets a day, and each data set is divided into 3 groups (training set, validation set, and prediction set) to conduct experiments; iv) based on the experimental tests, adaptive hyperparameters are established, and the smallest test set var_loss is used as the basis for early stopping. Among them, the specific hyperparameter settings are shown in Table 1; v) calculate the modeling and prediction accuracy.

Table 1. Location of 9 selected stations of CMONOC network

Number	Parameters	Value
1	Loss	MSE
2	Optimizer	Adam
3	Number of LSTM layers	3
4	Number of dense layers	1
5	Number of Epochs	50
6	Dropout value	0.2
7	Input dimension size	6
8	Output dimension size	1
9	Size of Batch	400
10	Validation split size	15:1
11	Initial learning rate	5×10^{-i}, $i = 2{:}1{:}7$
12	Early stopping	Monitor = val_loss; patience = 3

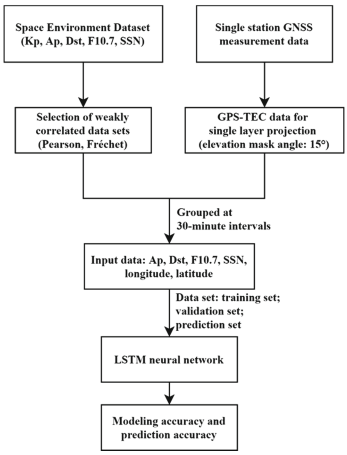

Fig. 3. Flow chart of LSTM model

After the models are well trained, the prediction results (predicted_i) of the models are compared with the TEC observation data (observed_i) of the stations respectively. Three performance indicators, mean absolute error (MAE), root mean square error (RMSE) and mean relative precision (P), are used to evaluate the performance of the model [20], which are calculated as shown in Eqs. 3, 4 and 5.

$$MAE = \frac{1}{N}\sum_{i=1}^{N}\left|\left(\text{observed}_i - \text{predicted}_i\right)\right| \tag{3}$$

$$RMSE = \sqrt{\frac{1}{N}\sum_{i=1}^{N}\left(\text{observed}_i - \text{predicted}_i\right)^2} \tag{4}$$

$$P = 1 - \sum_{i=1}^{n}\frac{\left|\text{observed}_i - \text{predicted}_i\right|}{\text{observed}_i} \tag{5}$$

4 Experiment and Analysis

The ionosphere shows complex spatial variations with latitude and longitude. To verify the adaptability and prediction accuracy of the prediction model at different spatial locations, three regions, low (0°–30°), mid (30°–45°), and high latitude (45°–60°), are divided to select stations respectively. In this paper, a total of 9 stations were selected for the experiment, and the GPS station locations and details are shown in Fig. 4 and Table 2, including 4 low-latitude stations, 3 mid-latitude stations and 2 high-latitude stations.

To represent the prediction accuracy every 30 min in more detail and intuitively, the error bars of each time period are plotted in this paper by combining the predicted MAE and RMSE values, as shown in Fig. 5. From Fig. 5(a), it can be seen that the errors of most time periods at low latitude stations are within 5 TECu. The forecast errors are larger in the 06:00 UTC-10:00 UTC (14:00 LT-18:00 LT) time period, especially for the KMIN station, where some anomalous continuous scatter points with large deviations can be found from Fig. 6(c), and thus may be associated with equatorial ionospheric anomalies (EIA) [21] at low latitudes. These anomalies differ from the modeled values by about 30 TECu, which in turn would enlarge the residual values during this time period.

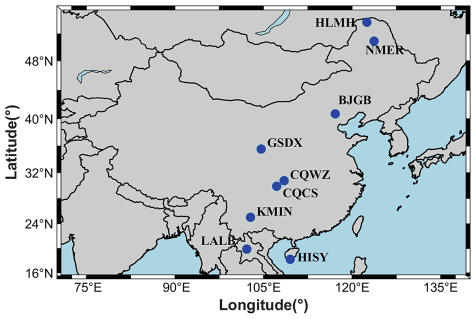

Fig. 4. The spatial distribution location of GPS stations

Figure 6 shows the predicted LSTM values of the four stations at low latitudes and the measured GPS TEC, IRI TEC and RIM TEC values, respectively. The measured data are selected to be within 3° difference in longitude and within 1° difference in latitude from the station coordinates.

Table 2. The results of 9 selected stations

Classification	Station name	Latitude (°N)	Longitude (°E)	Modeling accuracy		Prediction accuracy (TECu)		
				MAE	RMSE	MAE	RMSE	P (%)
Low latitude	HISY	18.236	109.531	5.983	2.918	2.918	2.245	83.5
	LALB	19.898	102.165	5.385	3.593	2.601	2.030	84.5
	KMIN	25.030	102.798	5.385	2.601	2.867	2.279	83.8
	CQCS	29.905	107.232	3.831	1.520	1.520	1.270	82.6
Middle latitude	CQWZ	30.770	108.490	3.377	3.066	1.427	1.260	81.0
	GSDX	35.554	104.605	2.379	2.073	1.047	0.829	84.0
	BJGB	40.692	117.158	1.989	1.292	0.884	0.642	83.8
High latitudes	NMER	50.576	123.727	1.915	1.167	0.971	0.655	71.7
	HLMH	52.975	122.513	1.522	1.012	0.828	0.618	81.9

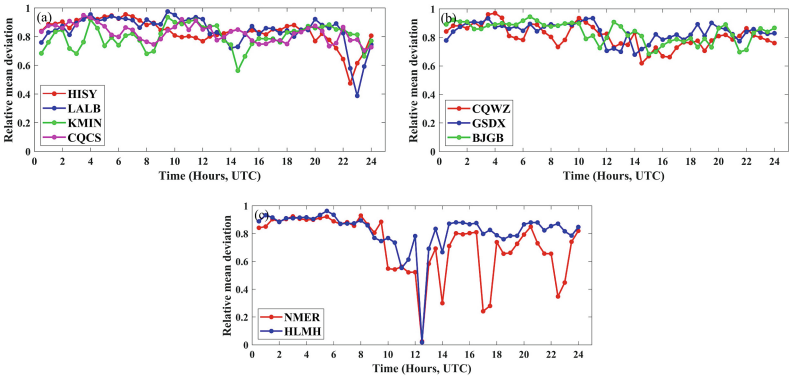

Fig. 5. The relative mean deviation of LSTM prediction; (a) low latitude station; (b) mid-latitude station; (c) high latitude station

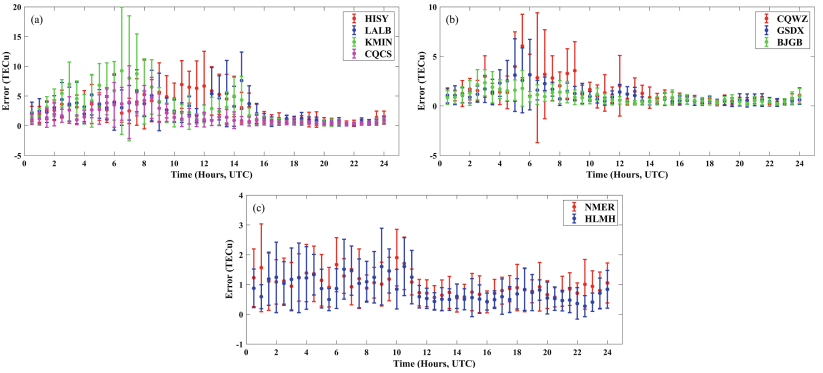

Fig. 6. The error bar of LSTM prediction; (a) low latitude station; (b) mid-latitude station; (c) high latitude station

From Fig. 6, it can be seen that: 1) the TEC tends to decrease with increasing latitude. Among them, the forecast values of the LSTM model agree well with the measured data, which means that the model can capture the changes of TEC well, and predict the low-latitude ionospheric TEC better with a residual of 2–5 TECu compared with the IRI2016 model and the CMONOC RIM; 2) the RIM data is overall more consistent with the measured data, but the TEC values are overestimated in the time period 04:00 UTC-08:00 UTC. Comparing Figs. 6(a–d), it can be found that this overestimation of the RIM is due to some anomalous values in this time period. The RIM value is closer to the measured value than the IRI model value, and the forecast effect is more stable; 3) The IRI2016 model captures only the general trend of TEC, and the IRI model forecasts poorer values from 06:00 UTC-10:00 UTC (14:00 LT-18:00 LT), which is consistent with the paper [22]. The difference between IRI and the measured data tends to increase with the increase of latitude. The IRI forecasts from 20:00 UTC-24:00 UTC (04:00 LT-08:00 LT) are better, and the forecast values are consistent with the measured data.

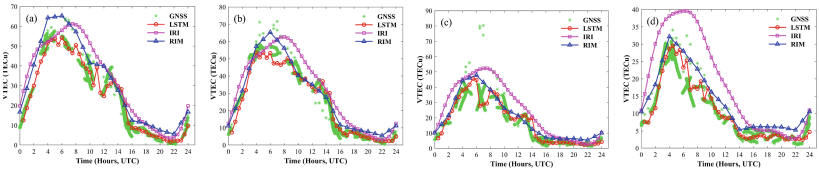

Fig. 7. Comparison of TEC values predicted by LSTM (red solid line) and IRI2016 (magenta solid line), and RIM (blue solid line) data and actual GPS data (green scatter) from low-latitude stations; (a) HISY; (b) LALB; (c) KMIN; (d) CQCS

Figure 7 shows the comparison of the LSTM forecast results of the stations in the mid-latitude region with other global ionospheric models and the measured data. The LSTM forecast data are in good agreement with the measured data and are not easily affected by the anomalous discrete points. The RIM data, however, overestimate TEC due to the influence of anomalous values. IRI data still have poor daytime forecasts and high forecast accuracy at night. Specifically, the forecast is poor from 02:00 UTC-10:00 UTC (10:00 LT-18:00 LT) and superior from 16:00 UTC-24:00 UTC (00:00 LT-08:00 LT), and its time length is extended compared to that at lower latitudes.

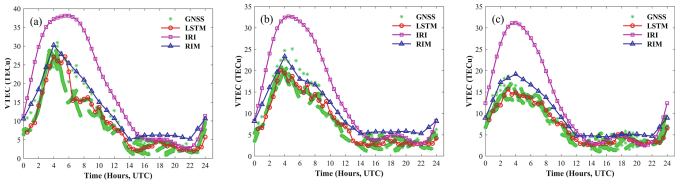

Fig. 8. Comparison of TEC values predicted by LSTM (red solid line) and IRI2016 (magenta solid line), and RIM (blue solid line) data and actual GPS data (green scatter) from mid-latitude stations; (a) CQWZ; (b) GSDX; (c) BJGB

The forecast results for the high latitude region are shown in Fig. 9, from which it can be seen that the GPS measured TEC values fluctuate between 1 and 5 TECu during the period of 12:00 UTC-23:00 UTC, and the points are more scattered. This results in the current situation that the LSTM model of NMER station forecasts TEC values with small MAE and RMSE but low relative accuracy, which explains the result in Fig. 5(c). The LSTM fits the measured data well throughout the time period, while the RIM data are slightly overestimated during the day and underestimated during the night.

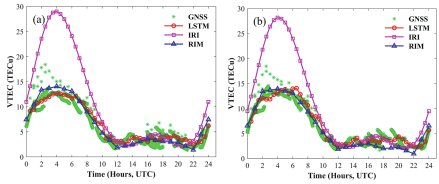

Fig. 9. Comparison of TEC values predicted by LSTM (red solid line) and IRI2016 (magenta solid line), and RIM (blue solid line) data and actual GPS data (green scatter) from high-latitude stations; (a) NMER; (b) HLMH

5 Conclusion

In this paper, single-station regional ionospheric models are constructed and forecasted by LSTM network method based on single-station GPS data from different regions (high, middle and low latitude regions) of China CMONOC network in 2014 as well as space environment data. The forecast results are compared and analyzed with the IRI2016 model, CMONOC-RIM data, and measured GPS data. The following conclusions were obtained: i) in terms of forecast accuracy, the MAE and RMSE are about 3 TECu and 2 TECu at low latitude, 2 TECu and 1 TECu at mid-latitude, and 1 TECu and 0.6 TECu at high latitude, and the relative accuracy of the low and mid-latitude stations are comparable, both around 82%, while their relative accuracy decreases at high latitude, which is about 70–80%. Overall, the time-phased LSTM single-station regional model is feasible and has high forecast accuracy; ii) geographically, the MAE and RMSE of the same longitude decrease with increasing latitude, and the MAE and RMSE of several stations in the low-latitude region are the largest and the smallest in the high-latitude region, mainly due to the different TEC content of the ionosphere at different latitudes [23]; iii) the LSTM model forecasts for stations at low, mid, and high latitudes are in good agreement with the measured data and can be less susceptible to anomalies; iv) the RIM data are generally consistent with the measured data, but the TEC values are overestimated during the daytime, and this overestimation is due to some anomalous values during this time period; v) the IRI model only captures the general trend of TEC. It forecasts poorly in the daytime, and its overestimation becomes more obvious as the latitude increases, but performs better in the evening.

Therefore, this study verifies that it is feasible to train the LSTM network forecast TEC using real measurement data in segments, and has a good forecast accuracy. This

paper lays the foundation for subsequent regional modeling and forecasting, and its LSTM forecast model can provide ionospheric constraint support for navigation.

Acknowledgments. This work was supported by Science and Technology Planning Project of Guangdong Province of China (Grant No. 2021A0505030030). The authors would like to thank CMONOC for GPS data (ftp.cgps.ac.cn/products/ionosphere/data). Kp, Dst indexes were downloaded from the website (http://isgi.unistra.fr/data_download.php/), and F10.7, SSN were downloaded from the (http://www.swpc.noaa.gov/wwire.html/).

References

1. Chen, W., Gao, S., Hu, C., Ding, C.X.: Effects of ionospheric disturbances on GPS observation in low latitude area. GPS Solut. (2008). https://doi.org/10.1007/s10291-007-0062-z
2. Yu, S., Liu, Z.: Feasibility analysis of GNSS-based ionospheric observation on a fast-moving train platform (GIFT). Satellite Navigation **2**(1), 1–18 (2021). https://doi.org/10.1186/s43020-021-00051-1
3. Tu, R., Zhang, R., Zhang, P., Han, J., Fan, L., Lu, X.: Recover the abnormal positioning, velocity and timing services caused by BDS satellite orbital maneuvers. Satellite Navigation **2**(1), 1–11 (2021). https://doi.org/10.1186/s43020-021-00048-w
4. Cai, C., Liu, L., Li, J., Liu, G.: Precision assessment of ionospheric delay calculated from improved Klobuchar model in China. J. Guilin. Univ. Technol. **37**, 120–124 (2017)
5. Wang, F., Wu, X., Zhou, T., Li, Y.: Performance comparison between different Klobuchar model parameters. Acta Geod Cartogr Sin (2014). https://doi.org/10.13485/j.cnki.11-2089.2014.0176
6. Wang, N., Yuan, Y., Li, Z., Li, M.: Performance analysis of different NeQuick ionospheric model parameters. Acta Geod Cartogr. Sin. **46**, 421–429 (2017)
7. Chen, J., Ren, X., Zhang, X., Zhang, J., Huang, L.: Assessment and Validation of Three Ionospheric Models (IRI-2016, NeQuick2, and IGS-GIM) From 2002 to 2018. Space Weather Int. J. Res. Appl. **18**, e2019SW002422 (2020)
8. Zhao, L., Yang, Z., Wu, X., Troops: temporal and spatial variation and perturbation analysis for China with GIM and IRI2012 model. Prog. Geophys. (2016)
9. Zhong, H., Xiao, Y., Feng, J., Zhu, Y.: Analysis of TEC prediction ability of IRI2016 model. Sci. Surv. Mapp. **46**, 54–66 (2021)
10. Ansari, K., Park, K.-D., Kubo, N.: Linear time-series modeling of the GNSS based TEC variations over Southwest Japan during 2011–2018 and comparison against ARMA and GIM models. Acta Astronaut. **165**, 248–258 (2019)
11. Li, L., Zhang, S., Wang, Y., Hu, Q., Yin, S.: Ionospheric total electron content prediction based on ARMA model. J. Basic Ence. Eng. **21**, 814–822 (2013)
12. Lu, T., Huang, J., Lu, C.: Short-term lonospheric TEC prediction model based on EWT-ARMA. J. Geod Geodyn. **41**, 331–335 (2021)
13. Liu, S., Cao, X., Li, C.: Prediction models of ionospheric TEC by EEMD and radial basis function neural network. Eng. Surv. Mapp. **29**, 15–19 (2020)
14. Ruwali, A., Kumar, A.J.S., Prakash, K.B., Sivavaraprasad, G., Ratnam, D.V.: Implementation of hybrid deep learning model (LSTM-CNN) for ionospheric TEC forecasting using GPS data. IEEE Geosci. Remote Sens. Lett. **18**, 1004–1008 (2021)
15. Kim, J., Kwak, Y., Kim, Y.H., Moon, S., Jeong, S., Yun, J.Y.: Regional ionospheric parameter estimation by assimilating the LSTM trained results Into the SAMI2 model. Space Weather (2020). https://doi.org/10.1029/2020SW002590

16. Kim, J., Kwak, Y., Kim, Y., Moon, S., Jeong, S., Yun, J.: Potential of regional ionosphere prediction using a long short-term memory deep-learning algorithm specialized for geomagnetic storm period. Space Weather (2021). https://doi.org/10.1029/2021SW002741
17. Xiong, P., Zhai, D., Long, C., Zhou, H., Zhang, X., Shen, X.: Long short-term memory neural network for ionospheric total electron content forecasting over China. Space Weather (2021). https://doi.org/10.1029/2020SW002706
18. Lai, Y., Yao, Y., Zhang, L.: Accuracy assessment of CODE GIM in China. J. Geomat. **46**, 8–12 (2021)
19. Wien, T.U., Eiter, T., Eiter, T., Mannila, H., Mannila, H.: Computing discrete Fréchet distance. See Also **64**, 636–637 (1994)
20. Yang, Y., Mao, Y., Sun, B.: Basic performance and future developments of BeiDou global navigation satellite system. Satellite Navigation **1**(1), 1–8 (2020). https://doi.org/10.1186/s43020-019-0006-0
21. Song, R., Zhang, X., Zhou, C., Liu, J., He, J.: Predicting TEC in China based on the neural networks optimized by genetic algorithm. Adv. Space Res. **62**, 745–759 (2018)
22. Zhang, T., Zhao, Q., Zhong, H., Zhang, Y.: Accuracy analysis of IRI 2016 model in ocean and land areas. Sci. Surv. Mapp. **46**, 14–33 (2021)
23. Huang, J., Lu, T., He, X., Li, W.: Short term Prediction model of ionospheric TEC based on residual correction of prophet-elman. J. Geod Geodyn. **41**, 783–788 (2021)